



UNIVERSITY OF LEEDS

This is a repository copy of *A multiphase seismic investigation of the shallow subduction zone, southern North Island, New Zealand*.

White Rose Research Online URL for this paper:
<http://eprints.whiterose.ac.uk/435/>

Article:

Reading, A.M., Gubbins, D. and Mao, W.J. (2001) A multiphase seismic investigation of the shallow subduction zone, southern North Island, New Zealand. *Geophysical Journal International*, 147 (1). pp. 215-226. ISSN 0956-540X

<https://doi.org/10.1046/j.1365-246X.2001.00500.x>

Reuse

See Attached

Takedown

If you consider content in White Rose Research Online to be in breach of UK law, please notify us by emailing eprints@whiterose.ac.uk including the URL of the record and the reason for the withdrawal request.



eprints@whiterose.ac.uk
<https://eprints.whiterose.ac.uk/>

A multiphase seismic investigation of the shallow subduction zone, southern North Island, New Zealand

Anya M. Reading,* David Gubbins and Weijian Mao†

Department of Earth Sciences, University of Leeds, Leeds, LS2 9JT, UK

Accepted 2001 April 30. Received 2001 March 19; in original form 2000 August 17

SUMMARY

The shallow structure of the Hikurangi margin, in particular the interface between the Australian Plate and the subducting Pacific Plate, is investigated using the traveltimes of direct and converted seismic phases from local earthquakes. Mode conversions take place as upgoing energy from earthquakes in the subducted slab crosses the plate interface. These *PS* and *SP* converted arrivals are observed as intermediate phases between the direct *P* and *S* waves. They place an additional constraint on the depth of the interface and enable the topography of the subducted plate to be mapped across the region.

301 suitable earthquakes were recorded by the Leeds (Tararua) broad-band seismic array, a temporary line of three-component short-period stations, and the permanent stations of the New Zealand national network. This provided coverage across the land area of southern North Island, New Zealand, at a total of 17 stations. Rays are traced through a structure parametrized using layered B-splines and the traveltime residuals inverted, simultaneously, for hypocentre relocation, interface depth and seismic velocity.

The results are consistent with sediment in the northeast of the study region and gentle topography on the subducting plate. This study and recent tectonic reconstructions of the southwest Pacific suggest that the subducting plate consists of captured, oceanic crust. The anomalous nature of this crust partly accounts for the unusual features of the Hikurangi margin, e.g. the shallow trench, in comparison with the subducting margin further north.

Key words: converted phase, Hikurangi margin, New Zealand, plate topography, subduction zone.

1 INTRODUCTION

Converted mode energy, occurring on seismic records from southern North Island, New Zealand, is used in this study to enable the nature and topography of the interface between the two converging plates to be investigated in greater detail than is possible using only direct seismic waves. Traveltime residuals are inverted for the seismic velocity, converting interface depth and hypocentre location of the shallow (< 100 km) part of the Hikurangi margin. We aim to determine an improved seismic structure for this anomalous and transitional region.

1.1 Tectonic setting

The Hikurangi margin (Fig. 1a) is the southernmost expression of the Tonga–Kermadec subduction zone of the southwest

Pacific. Relative plate motions (Walcott 1987) and the north-west-dipping Wadati–Benioff zone (Robinson 1986) confirm that the Pacific plate is rotating and undergoing oblique subduction beneath the Indian–Australian Plate (subsequently referred to as ‘Australian’). The Hikurangi Trough, less well pronounced than the Kermadec Trench, is the surface expression of the plate boundary south of 36°S. Down the Hikurangi margin, convergence between the plates decreases until at approximately 42°S, strike-slip motion dominates and subduction no longer occurs. Relative motion between the plates is taken up in the Southern Alpine fault zone of the South Island, while south of New Zealand, the Australian plate is subducting under the Pacific plate. The Hikurangi margin is thus a transitional region between the fast ocean–ocean subduction of the Kermadec trench and the intracontinental strike-slip of South Island.

The estimated volume of sediment transported to the trench exceeds that of the frontal wedge associated with the subduction zone (Bradshaw 1989). It is therefore likely that a proportion of sediment arriving at the Hikurangi Trough is subducted (Walcott 1987). This is supported by gravity (Smith *et al.* 1989) and seismic (Bannister 1988; Eberhart-Phillips & Reyners 1999)

* Now at: Research School of Earth Sciences, Australian National University, Canberra, ACT 0200, Australia. E-mail: anya@rsees.anu.edu.au

† Now at: Western Geophysical, 455 London Road, Isleworth, Middlesex, TW7 5AB, UK

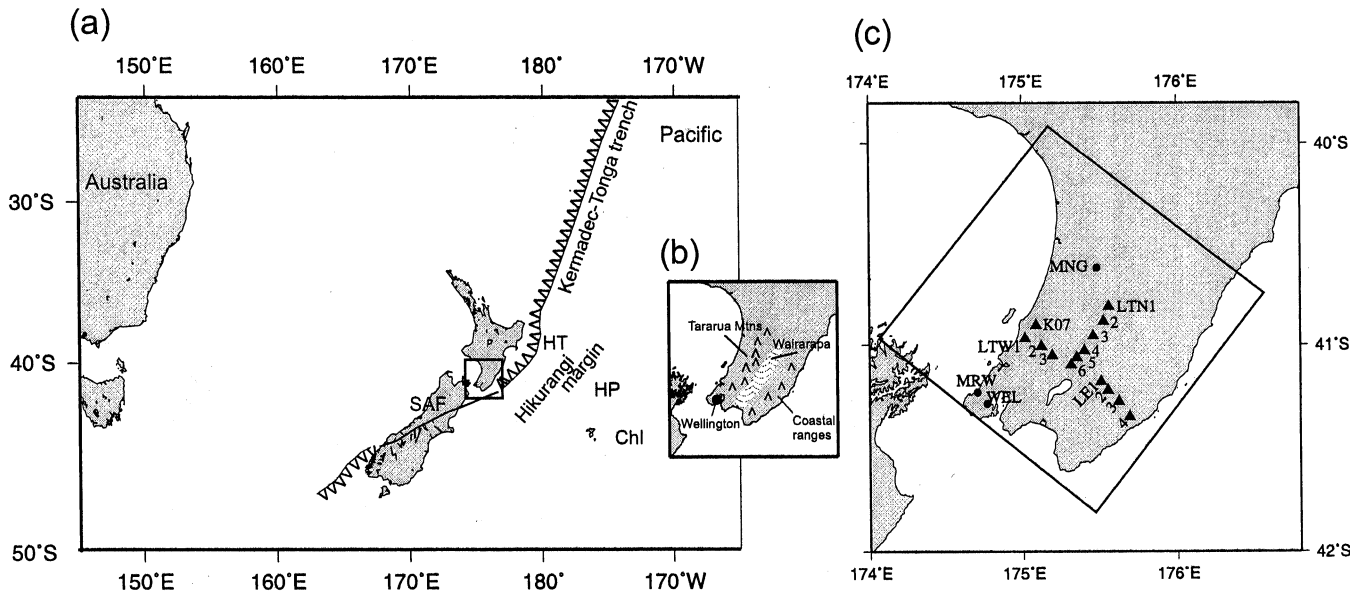


Figure 1. (a) The tectonic setting of New Zealand showing convergent plate margins to the north and south and the strike-slip regime through the Alpine Fault of the Southern Alps. SAF: Southern Alpine Fault; HT: Hikurangi Trough; HP: Hikurangi Plateau; ChI: Chatham Islands. (b) The main geographical divisions of the area studied in this work. (c) Map of the study area (boxed) in southern North Island, New Zealand, and seismic stations used. LTW: Leeds Tararua West; LTN: Leeds Tararua North; MNG, MRW and WEL: New Zealand National Network stations operated by IGNS.

modelling of the structure of northern North Island. Given the topography on the Hikurangi Plateau to the east of the Trough, it is likely that the subducted sediment is distributed unevenly along the strike of the subduction zone.

The subducting oceanic crust is anomalous following the change in plate configuration off the west coast of what is now New Zealand during the Cretaceous. The approaching Pacific–Phoenix spreading ridge (Bradshaw 1989) stopped short of the trench (Luyendyk 1995), the downgoing plate being too young and small to subduct, and welded to the outer plate over the dormant spreading centre. The Phoenix Plate then took on the motion of the Pacific Plate, shutting down both subduction and spreading between 110 and 105 Ma (Fig. 2). This change in regime facilitated the creation of an anomalously thick oceanic crust, part of which is currently being subducted underneath northern North Island. This region, known as the Hikurangi Plateau, has been extensively investigated using seismic and potential means. It shows structural features such as basins and areas of volcanism that support this hypothesis (Wood & Davy 1994; Davy & Wood 1994).

1.2 Observed converted phases in New Zealand

Converted phases have been observed in New Zealand from the 1960s (Smith 1970) through to the present day. Ansell & Bannister (1996), and references therein, summarize recent microearthquake studies with frequent observations of energy arriving between the direct *P* and *S* waves. They also summarize the relative lack of earthquakes with focal mechanisms that indicate thrust faulting near the plate interface. Such earthquakes are important in deducing subduction zone structure since they are likely to occur at asperities between the two plates and hence define the plate interface. In New Zealand, where few thrust events occur, analysis of converted phases provides an alternative way of studying the plate boundary region.

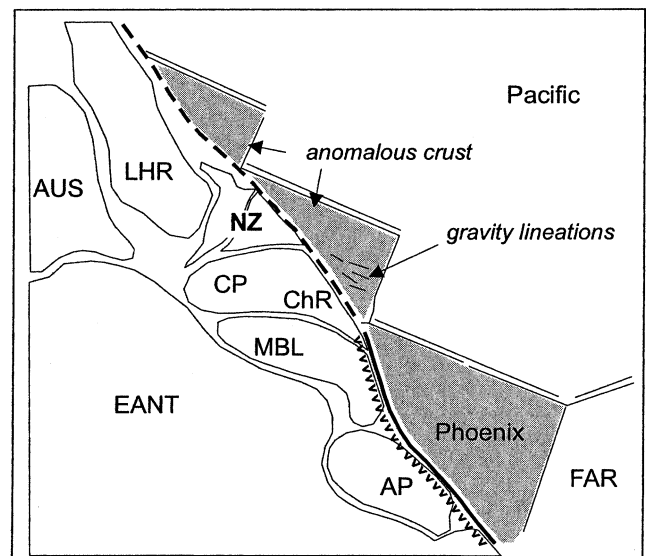


Figure 2. Plate reconstruction *c.* 105 Ma showing plate capture and the formation of anomalous crust between the Pacific and Phoenix Plates. EANT: East Antarctic Plate; AUS: Australian Plate; FAR: Farallon Plate; LHR: Lord Howe Rise; NZ: New Zealand block; CP: Campbell Plateau; ChR: Chatham Rise; MBL: Marie Byrd Land; AP: Antarctic Peninsula (simplified from Luyendyk 1995).

1.3 B-spline parametrizations

B-splines are capable of representing structures such as the major element of a subduction zone, a dipping interface, better than most block parametrizations. The seismic structure is parametrized in terms of layers, each layer interface being described by a 2-D B-spline function (Powell 1991; Lancaster & Salkauskas 1986). Similar functions are also used to represent the horizontal variations of velocity within each layer, including the strong lateral velocity variations that are a feature of

destructive plate margins. B-spline parametrizations are computationally efficient and, being locally supported, allow straightforward calculation of B-spline functions and their first and second derivatives (de Boor 1972; Bray 1991) via recurrence relations.

1.4 Inversion

The inversion scheme broadly follows the stochastic inverse method for the simultaneous determination of structure and hypocentre parameters outlined by Spencer & Gubbins (1980). In most previous work, including Spencer & Gubbins (1980), only slowness or velocity is included in the structure parametrization. In this work we invert for both improved seismic velocity and the depth of the converting interface, and the term *structure parameters* will be used for variables describing both velocity and interface depth.

The stochastic inverse (Franklin 1970) provides a means of coping with non-resolvable parts of the problem without eigenvector analysis. The basic equation,

$$\mathbf{T} = \mathbf{A}\mathbf{v} + \mathbf{B}\mathbf{h} + \boldsymbol{\varepsilon}, \quad (1)$$

is to be solved for minimum error, $\boldsymbol{\varepsilon}$, where \mathbf{T} is the vector of traveltimes residuals, \mathbf{A} is a matrix of structure partial derivatives, \mathbf{B} is a matrix of hypocentre partial derivatives, \mathbf{v} is a vector of structure parameter perturbations and \mathbf{h} is a vector of hypocentre perturbations.

The normal equations, which give the condition for the required minimum, are

$$\mathbf{A}^T\mathbf{T} = \mathbf{A}^T\mathbf{A}\mathbf{v} + \mathbf{A}^T\mathbf{B}\mathbf{h}, \quad (2)$$

$$\mathbf{B}^T\mathbf{T} = \mathbf{B}^T\mathbf{A}\mathbf{v} + \mathbf{B}^T\mathbf{B}\mathbf{h}.$$

For the stochastic inverse, the problem is re-posed using damping terms d and e , which confine the structure and hypocentre parts of the problem respectively. The damped analogues of the normal equations are

$$\mathbf{A}^T\mathbf{T} = (\mathbf{A}^T\mathbf{A} + d\mathbf{W}^{-1})\mathbf{v} + \mathbf{A}^T\mathbf{B}\mathbf{h}, \quad (3)$$

$$\mathbf{B}^T\mathbf{T} = (\mathbf{B}^T\mathbf{A} + e\mathbf{Q}^{-1})\mathbf{v} + \mathbf{B}^T\mathbf{B}\mathbf{h},$$

where \mathbf{W} and \mathbf{Q} are covariance matrices of structure and hypocentre parameters respectively. By varying d and e between zero and very large values it is possible to view the problem as a simple inversion for structure ($e = \infty$), a hypocentre relocation problem ($d = \infty$), or a compromise between the two. The required hypocentre and structure parameters are then found:

$$\mathbf{h} = (\mathbf{B}^T\mathbf{B} + e\mathbf{Q}^{-1})^{-1}(\mathbf{B}^T\mathbf{T} - \mathbf{B}^T\mathbf{A}\mathbf{v}),$$

$$\mathbf{v} = (\mathbf{O}\mathbf{A} + d\mathbf{W}^{-1})^{-1}(\mathbf{O}\mathbf{T}), \quad (4)$$

$$\text{where } \mathbf{O} = \mathbf{A}^T - \mathbf{A}^T\mathbf{B}(\mathbf{B}^T\mathbf{B} + e\mathbf{Q}^{-1})^{-1}\mathbf{B}^T.$$

2 DATA

2.1 Array

The Leeds Tararua (LT) broad-band array (Stuart *et al.* 1995) was extended using short-period installations (the Leeds East, LE, line) in order to increase coverage perpendicular to the strike of the subducting plate. The deployment extended coverage

from the Tararua mountains (Fig. 1b) across the Wairarapa to the (east) coastal ranges. Data from these three-component temporary stations were augmented by records from the nearby, permanent, three-component stations of the New Zealand network (Fig. 1c) that were operational at the time of the study. Single-component stations were not used since the methods in this study require three-component data. During the period of data acquisition, 301 earthquakes, recorded by the LT array and at least two stations of the LE line, occurred within the 150×150 km study region. This is shown as the box in Fig. 1(c). It is oriented with sides parallel to the dip of the subducting slab as determined by Robinson (1986). All earthquakes used in this work were assigned locations by the New Zealand Institute for Geological and Nuclear Sciences (IGNS). These were used as the starting locations for earthquakes in the simultaneous inversion.

2.2 Automatic picking of direct and converted seismic phases

Although converted phases were clearly observed on recordings made during the experiment (Fig. 3 shows a good example), many more exist but are difficult to pick above the P -wave coda. Reading *et al.* (2001), in the companion Research Note to this work, describe a method of enhancing converted phase yield through polarization filtering (Samson & Olson 1981) and the use of an automatic picking process for the direct and converted arrivals. In comparison to carefully manually picked data, the polarization-filtered and automatically picked data showed better S -wave pick accuracy, a dramatic improvement in PS yield and a considerable improvement in SP yield. The traveltimes in this work were therefore automatically picked, using this method and checked manually.

2.3 Traveltimes residuals

The source of mode conversions giving rise to the observed intermediate phases was determined through a pilot study (Reading 1996). Traveltimes of direct and converted waves from 14 earthquakes falling close to a line through the LE and LTW stations were found by ray tracing through a 2-D structure including the slab interface as a converting boundary. In a similar manner to Iidaka *et al.* (1990), it was deduced that the mode conversion took place at the upper surface of the subducted plate. There was no indication that a boundary at any other depth could account for the observed intermediate arrivals.

Direct and converted traveltimes for the main study were calculated by tracing rays through the layered model structure parametrized in terms of B-splines using the method of Mao & Stuart (1997). This technique is directed specifically towards the efficient calculation of traveltimes, and traveltimes partial derivatives with respect to the velocity and interface parameters, for subsequent use in the inversion routine. It is particularly suited to the improved determination of structure in the region of a major seismic discontinuity.

The traveltimes residuals, $t_{\text{obs}} - t_{\text{mod}}$, that is, the difference between the observed traveltimes and that calculated from the initial input model, are shown in a later section. Station elevations are included in the ray tracing, and the stations are all located on basement rock so there is no requirement for separate 'station terms'.

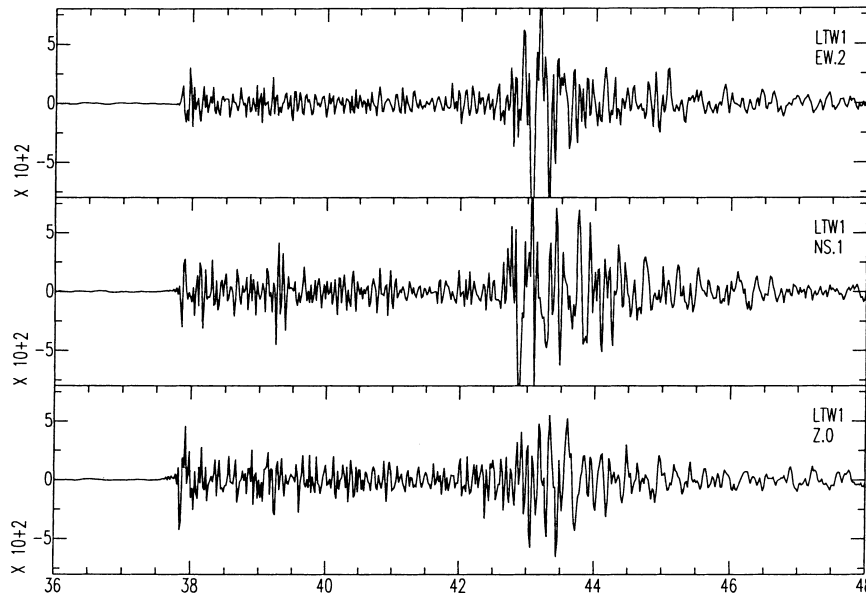


Figure 3. A good example of a *PS* converted phase recorded at station LTW1 (1992:03:06, 07:23:28.82). The three components are shown: east (upper), north (middle) and vertical (lower) with the converted mode energy clearest on the north component at just after 39 s from the start of the file.

2.4 Ray paths and sampling of structure

The ray paths through the initial model give very good coverage of the centre of the study box (Fig. 4 plan view) and, in particular, the region of the top of the subducted slab (see the cross-section, Fig. 4). There is a small gap, in the top 5 km, between LT-array and LE-array stations ($90 < x < 105$ km) corresponding to the Quaternary alluvial deposits of the Wairarapa, where there is no rock exposure and hence no suitable site for a temporary seismic station. The edges of the model are poorly sampled, especially to the northwest and northeast.

The plate–plate interface is well sampled in the central region of the study area, by both direct and converted phases. In Fig. 5, symbols are plotted where the rays meet the top of the subducting plate; direct waves are shown in black and the conversion points of *SP* and *PS* phases in white. Again the edge of the study box is not sampled well enough for improved determinations of interface depth to be made in these regions. The data distribution also implies that it is not possible to constrain the hypocentre locations of earthquakes at the edge of the study better than the determinations made by the New Zealand IGNS.

3 METHOD

3.1 Model parametrization

The initial 2-D model used in this work is shown in cross-section in Fig. 6. It extends over the boxed region shown in Fig. 1(c), is based on Robinson (1986) and Ansell & Bannister (1996), and consists of five dipping layers in which the velocity varies down-dip. The converting interface is between layers 4 and 5. During the inversion, velocity parameters within each layer are allowed to vary both down-dip and along the strike of the subducted plate. Perturbations to the depth of the converting interface are also solved for but the other layer boundaries are fixed.

The seismic velocities and depths of the five layers are parametrized in terms of 2-D B-splines. The B-spline functions are expressed as a linear combination of B-spline basis functions (Powell 1991) and interpolate between knot points of specified layer depth to form surfaces approximating the layer boundaries. In a similar manner, the lateral variation of velocity within each layer is expressed by a 2-D B-spline function. The depth of the converting interface, between the fourth and fifth layers, is solved for in the subsequent inversion. The other interfaces are fixed at their *a priori* depths. There is no velocity variation with depth in a single layer, and *P* and *S* velocities are in a fixed ratio (that is, *S* velocities are not inverted for separately).

3.2 Weighting and damping

The timing at the field stations was carefully monitored and the arrival times automatically picked and checked with the need for accuracy in mind. In the case of anomalous, large residuals, invariably an incorrect event correlation had been made and the pick was not included in the inversion. Timing errors are uncorrelated, so T_{ij} are weighted using a diagonal matrix with elements equal to $1/\text{error}$ for that datum. Errors are assigned on the basis of phase, with *P*, *S* and converted phases at 0.6, 0.7 and 0.9 s respectively.

Damping is applied to the structural parameters, that is, the B-spline coefficients describing (a) the seismic velocities and (b) the converting interface. The relative damping of velocity and interface depth values within the same normal equations matrix is controlled by a ratio such that both velocity and interface parameters are allowed equal freedom during the inversion process. The structural parameters consist of both velocity values in the range 4.0 to 9.0 km s⁻¹ and depth parameters with different dimensions and values between 14.0 and 70.0 km. In practice, this leads to a change in damping parameter applied to the diagonal value of the normal equations matrix. The interface damping parameter is specified as a ratio of that applied to the velocities. In this way, the overall damping applied to the inversion may be changed without changing the relative damping of the velocity and interface parameters.

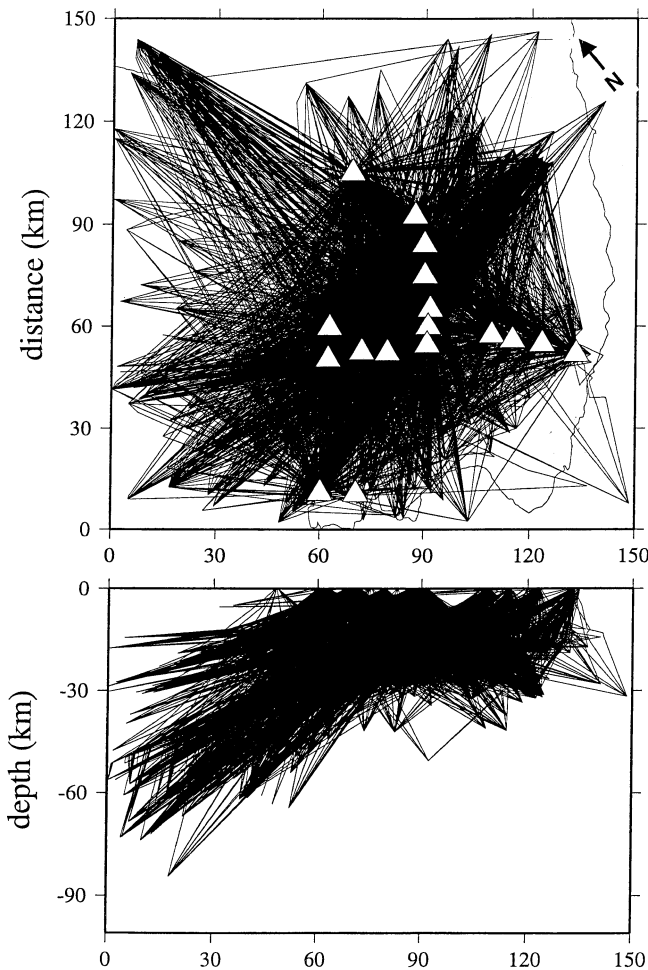


Figure 4. Plan (upper diagram) and cross-section (lower) of the source–receiver paths used in the inversion. Note the poorly sampled edges in the plan view and the dense sampling of the slab interface in the cross-section. The plan view shown here and in subsequent figures is of the study box indicated in Fig. 1(c), oriented as shown by the north arrow. The cross-sections are x versus depth plots of the same box, such that the slab dips from right to left. White triangles mark the recording stations.

The location given by the New Zealand IGNS for each event used in the inversion is critically assessed. In general, relocation is necessary, since an average 1-D model was used in the first determination of hypocentres by the New Zealand IGNS at the time of the experiment. Most of the events used were free to relocate in accordance with the least-squares minimization of traveltimes residuals. However, some poorly constrained earthquakes located on the edges of the modelled area are fixed in their original positions by adding a large number to the relevant element of the \mathbf{B} matrix. This damps out all perturbations to the parameter corresponding to this matrix element; that is, the parameter is not included in the inversion.

4 RESULTS

4.1 Reduction in residual traveltimes

The simultaneous inversion for perturbations to the original velocity model, converting interface and hypocentre locations resulted in a total reduction in root-mean-squared residuals of

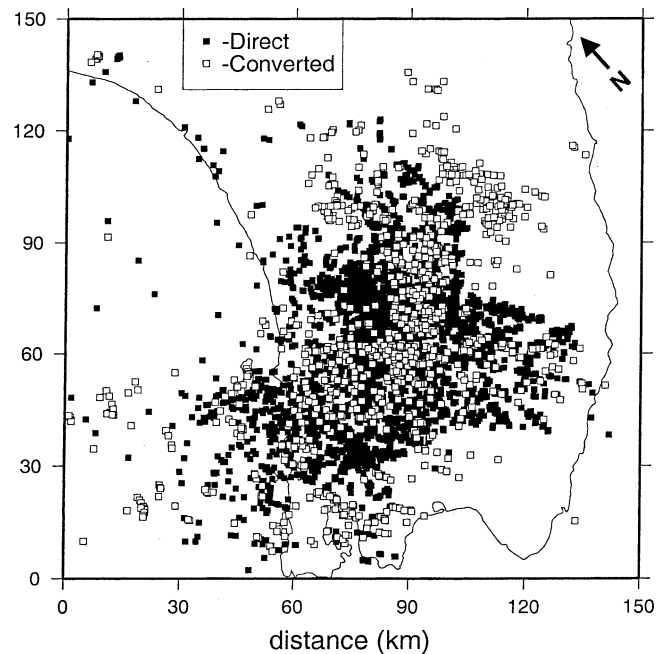


Figure 5. Plan-view of direct and converted ray intersection points (overlain) at the converting interface. The area shown is that of the box in Fig. 1(c).

19 per cent after the first iteration. A second iteration made a small additional improvement to a 20 per cent reduction in residuals in comparison to the original parameters. Third and subsequent iterations gave very small further improvements. P , S , SP and PS distributions of residuals have all been improved in a least-squares sense (Fig. 7). The bell-shaped distributions are clearly narrowed and, in the case of the S waves, become more symmetrical. The SP residual distribution after inversion peaks closer to zero and the PS distribution is now symmetrical—the remaining model errors being due to geological features beyond the resolution of this inversion scheme. The perturbed model describes the velocity and interface structure considerably better than the initial model.

Seismic anisotropy is a source of scatter in the S -wave plots. In the shallow region between the sources and receivers in this

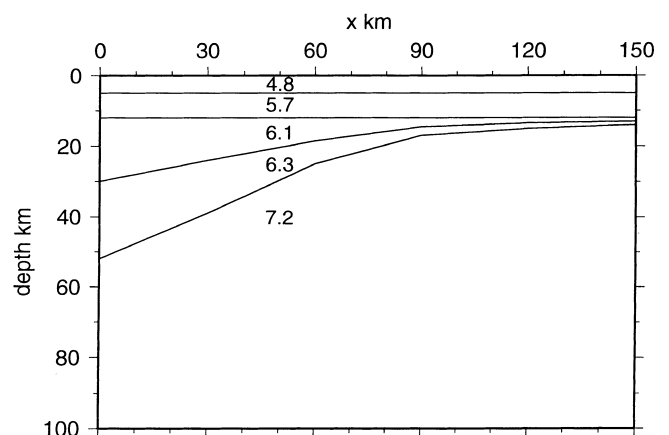


Figure 6. Input model: cross-section through the area of the upper Hikurangi subducting margin investigated in this study (Fig. 1c). It is parametrized in two dimensions for input into the inversion routine but is allowed to vary in three dimensions during inversion. Numbers show the input seismic velocity for each layer in km s^{-1} .

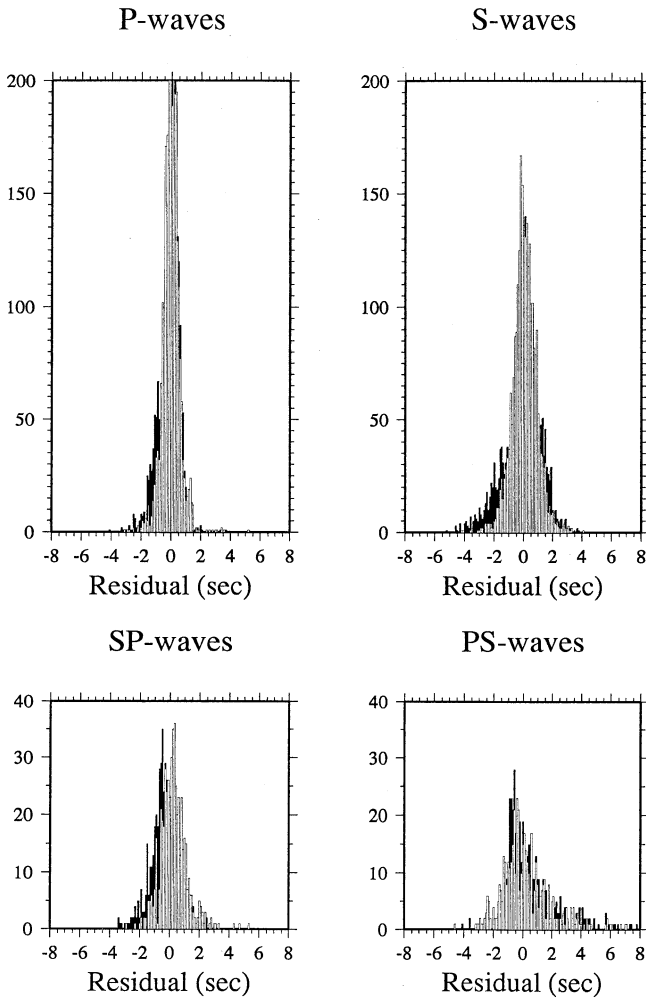


Figure 7. Histograms of residuals for direct and converted phases after inversion (white bars) plotted over those before inversion (black bars).

study the effects are largely unsystematic (Gledhill & Stuart 1996) and have not been accounted for in this study. Large-scale studies of seismic anisotropy in North Island (Brisbourne *et al.* 1999) do not have the required small-scale detail to be able to correct the *S*-wave traveltimes of this study but recent work on deeper sources of anisotropy (Marson-Pidgeon *et al.* 1999) is likely to be extended to the shallow crust in southern North Island in the future.

4.2 Velocity structure

The velocity structure is shown for each of the five layers of the best-fitting output model (Figs 8a–e). The figures should be viewed keeping in mind the regions of poor sampling (Fig. 4) where the structure is crossed by only a few rays. The depths of layers 1, 2 and 3 are the same as in the input model (Fig. 6) and the interface depth between layers 4 and 5 is discussed in the next section. All the layers exhibit an increase in velocity moving southeast to northwest, that is, the down-dip direction of the slab (right to left in Fig. 8). For the shallow layers, this reflects the convergent margin terranes observed at the surface continuing down into the crust according to the dominant structural lineation of the Hikurangi margin. For the deeper, dipping layers it reflects the increase in seismic velocity with depth. Layers 1–4 also show a velocity decrease along the strike of the subducted plate towards the southwest (the bottom of the plots in Fig. 8). This is a departure from 2-D symmetry in the overlying plate at mid-crustal depth and may represent the start of the transition from subduction to oblique transform faulting. The similarity between layers implies that factors causing lateral velocity variations act throughout the depth of the overriding plate. The actual layer boundaries between layers 2 and 3 and layers 3 and 4 are not geologically significant but allow a realistic velocity increase with depth to be modelled. Layer 5 (the subducted slab) shows little or no velocity variation along strike (top to bottom in Fig. 8).

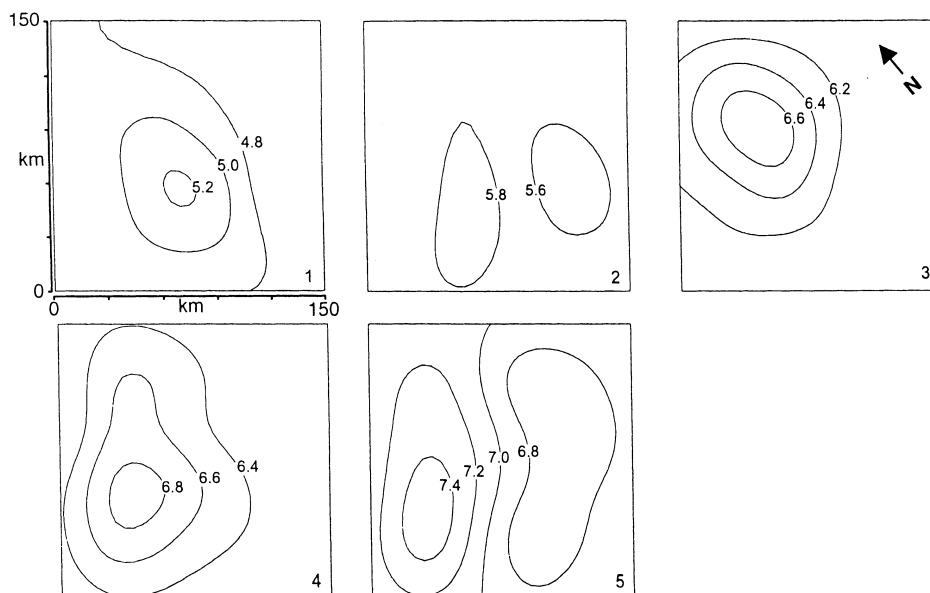


Figure 8. Velocity structure of layers 1–5 of the best-fitting output model (layer 1 being the shallowest) corresponding to the dipping layers of the input model shown in Fig. 6. Layer numbers are given in the bottom right-hand corner of each frame and the converting interface is between layers 4 and 5. Contour labels show the seismic velocity in each layer in km s^{-1} .

4.3 Converting interface

The best-fit perturbations to the interface parameters indicate that the converting boundary dips towards the northwest, starting at a very shallow angle, steepening at $x < 60$. The shallow part of this interface contains a broad depression, 2–4 km deep to the north of the LE array and east of the LT array. This is shown as a contour plot (Fig. 9). As illustrated in the plan view (Fig. 4), the region to the south of the depression, and hence the converting interface topography in that area, is not well sampled. To the north, the interface is better sampled. In the interpretation and discussion that follows, the essential feature is a shallow-angle converting interface corresponding to the north side of the depression.

4.4 Hypocentre relocation

Fig. 10 shows the hypocentre relocation vectors that best fit the data according to the results of this inversion. Events towards the northeast and northwest edges are fixed since they are not constrained by the station distribution of this experiment. The relocation of the events in plan view shows little systematic perturbation; however, in cross-section there is a general movement towards greater depth and towards the southeast (to the right of Fig. 10) shown by deeper events in the region $20 < x < 70$. Two more shallow clusters also show a systematic perturbation: a cluster around $x = 90$ moves to shallower depths above the slab whilst the events $100 < x < 130$ are perturbed such that the relocated hypocentres lie within the denser region of seismic activity near the top of the subducted slab. In the rare case that an earthquake with a recorded converted phase is relocated above the slab, the converted ray will fail to trace on the next iteration. In this case the arrival is

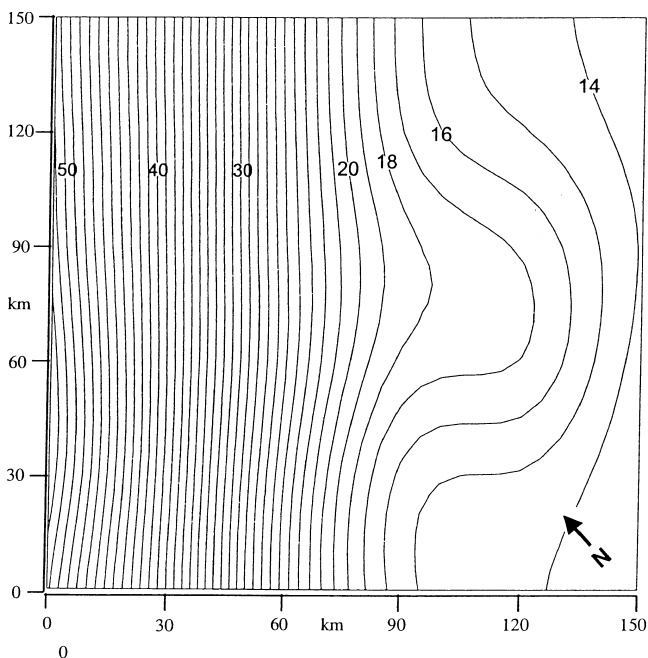


Figure 9. Contour plot of the converting interface—the depression in the interface can be clearly seen. Numbers indicate contour depths in km.

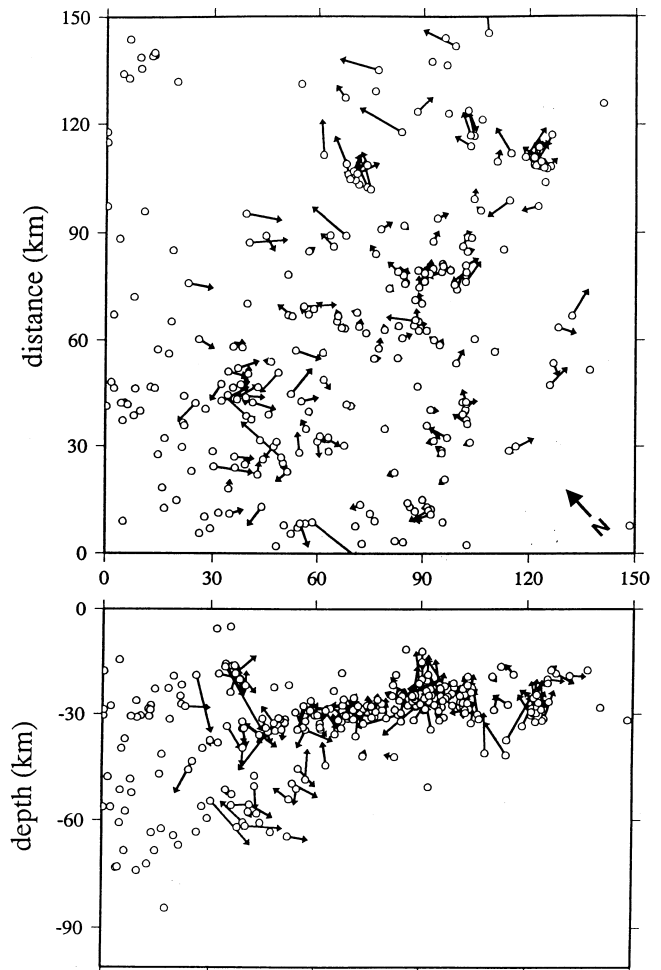


Figure 10. Plan view and cross-section of the earthquake hypocentre relocation vectors. The initial location is denoted by an open circle, and the final location by the arrow tip.

probably a reflected phase that has been misidentified. Fixing the hypocentres has the effect of mapping traveltimе perturbations into the velocity or interface structure.

4.5 Inversion validation

Figs 11(a) and (b) show the resolution and covariance matrices. The model resolution matrix is reasonably close to the ideal of large diagonal elements and zero off-diagonal elements, indicating that the model provided by the inversion process is a good estimate of the true model. The covariance matrix shows considerable off-diagonal elements. These are due to the trade-off between interface depth and velocity; that is, real velocity and/or depth variations may map to apparent depth and/or velocity variations in the final model. They may be interpreted as an indication of the need to consider the variations in interface depth as part of the perturbations to the structural parameters. Without the information inherent in converted phase arrivals and the inclusion of interface parameters, the perturbations are necessarily, and perhaps inappropriately, made to the velocity structure alone. In this case, damping ratios between the velocity and interface parameters are used that result in a geologically feasible velocity solution with the interface parameters perturbed accordingly.

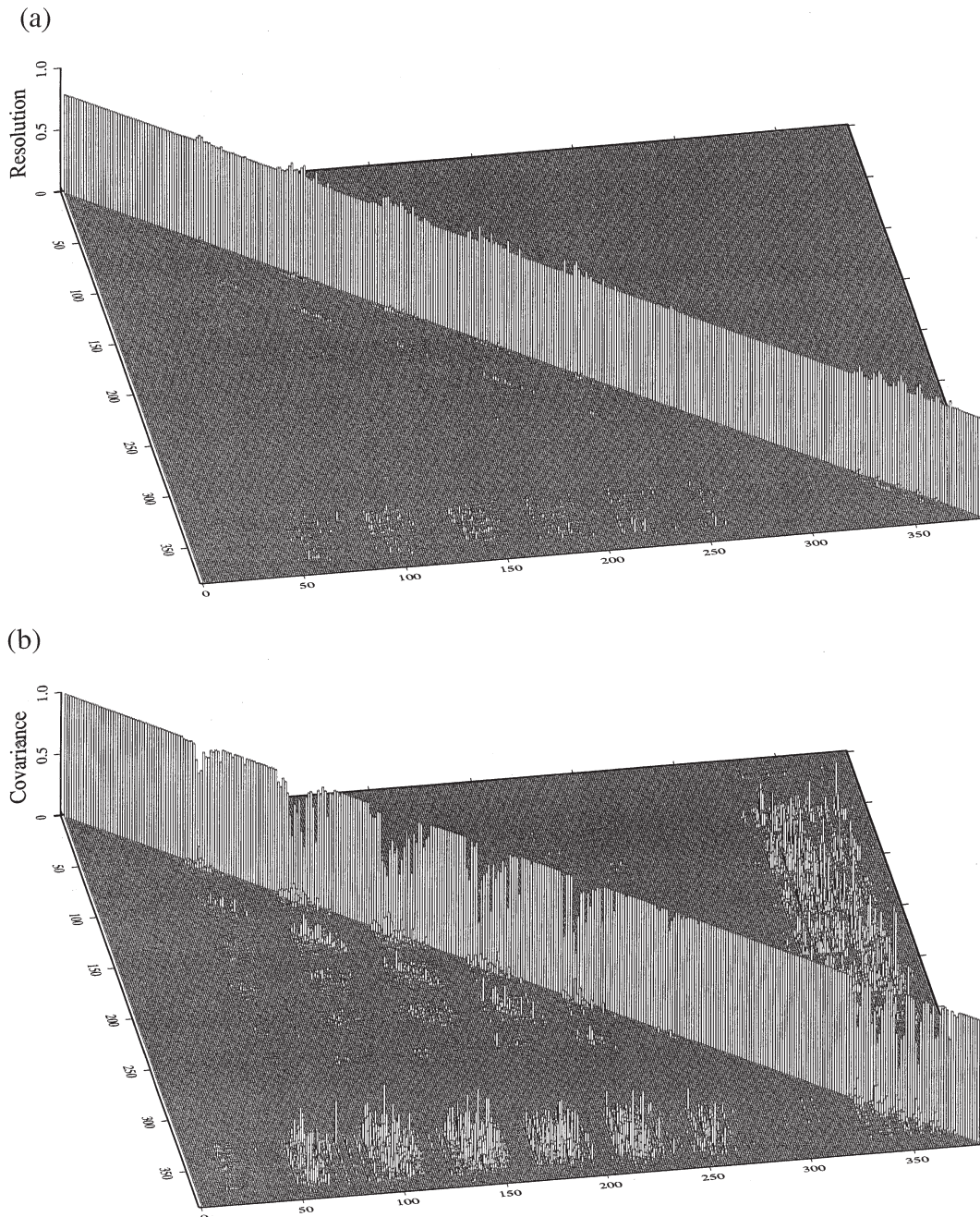


Figure 11. Model (a) resolution and (b) covariance matrices for the inversion.

5 INTERPRETATION

5.1 The distribution of subducted sediments

Walcott (1987) suggests that underplated sediments are an important feature of subduction at the Hikurangi margin. Sediment at the plate interface would enhance the impedance contrast and hence the amplitude of converted-mode waves produced at the interface. The amplitude ratio of converted energy to direct energy (Aki & Richards 1980) is high for the case $v_2 < v_1$, that is, the layer of the incident ray at the converting interface has a lower seismic velocity than the one above. It is reasonable, therefore, that areas with a high incidence of

converted phases in North Island, New Zealand, could be caused by subducted sediments at the plate boundary zone.

Clusters of phase conversions (Fig. 5) occur most notably down the northwest side and in the northeast. This distribution is subject to ray-geometry bias. *SP* arrivals sample the converting interface on the source side of the path. Since the stations are in the centre of the study area and the sources are widely scattered, more conversions are likely around the edges. Much of the high incidence of converted phases on the western edge is therefore due to source–receiver geometry. The high-incidence patch to the northeast, however, remains a very strong feature. There is no evidence from this study for subducted sediment across the Tararua region. In the northern Wairarapa,

the high incidence of converted phases suggests that this could be the southernmost extremity of underplated sediments. In order for sediments to be 'seen' by waves generated by earthquakes, the thickness of the sediment must be greater than 2 km. This patchy sediment distribution fits well between the deductions that the plates are well locked in northern South Island (Eberhart-Phillips & Reyners 1997) but that a low-velocity layer (subducted sediment) may be resolved in the northeast of North Island (Eberhart-Phillips & Reyners 1999). Between the end-member cases of a sediment-free interface under Cook Strait and a continuous sediment layer under East Cape, the thinner sediments under the area examined in this paper are distributed according to the topography of the plate interface zone. This result is consistent with the findings of Smith *et al.* (1989), who modelled Bouguer anomalies across the North Island. Short-wavelength features that fit well to an underplated sediment layer occur in a profile from Hawkes Bay but not in the more southerly Tararua region. It is possible that the converted phases in the northeast of the study area in this work correspond to the southern extremity of the sediments, which would account for the short-wavelength anomalies near Hawkes Bay. Geodetic modelling (Walcott 1987) requires sediment underplating to account for observed uplift, which concurs with this hypothesis. However, anomalous thickening (Luyendyk 1995) of the subducting crust could partly account for the long-wavelength component of this uplift.

Converted phase amplitudes could also be enhanced by layering at the interface (Helffrich & Stein 1993) and high converted phase yield may suggest the occurrence of laminated structures (rather than subducted sediment) at those regions of the plate boundary where this is observed. Mineral phase transitions within the subducted slab occur too deep to affect this study (Helffrich *et al.* 1989; Gubbins *et al.* 1994). It is therefore unlikely that the structure of the subducted slab itself (Smith *et al.* 1994; Lodge *et al.* 1999) causes variations in converted phase incidence on this relatively small scale. Heterogeneity along the plate boundary remains the most likely cause of the variation in the observed amplitudes.

5.2 Topography on the converting interface

The dominant feature of the converting interface is a broad, shallow (maximum amplitude 2–4 km) deepening of the interface over the eastern, shallower part of the slab between the values $y=30$ and $y=110$ (Fig. 9). In comparison with the offshore area of the Hikurangi margin, the spatial extent and wavelength of this depression is similar to, say, the 'Central Basin' of Wood & Davy (1994). It could either have existed as a topographic feature prior to subduction or be a response to compressional forces acting along the strike of the plate during and after subduction. There is no obvious correlation with surface geology. The depression is consistent with the summary diagram of Smith *et al.* (1989) who review the median depths of seismicity associated with the subducted slab. Their depth contours across the Wairarapa are approximately 4 km deeper than immediately to the north and south. If the high incidence of converted phases in the northeast of the study area is an indication of underplated sediment, this would correlate with the topography observed on the converting interface as shown (Fig. 12). In the region of subducted sediment, the high predicted amplitude for phases converted at the interface passing

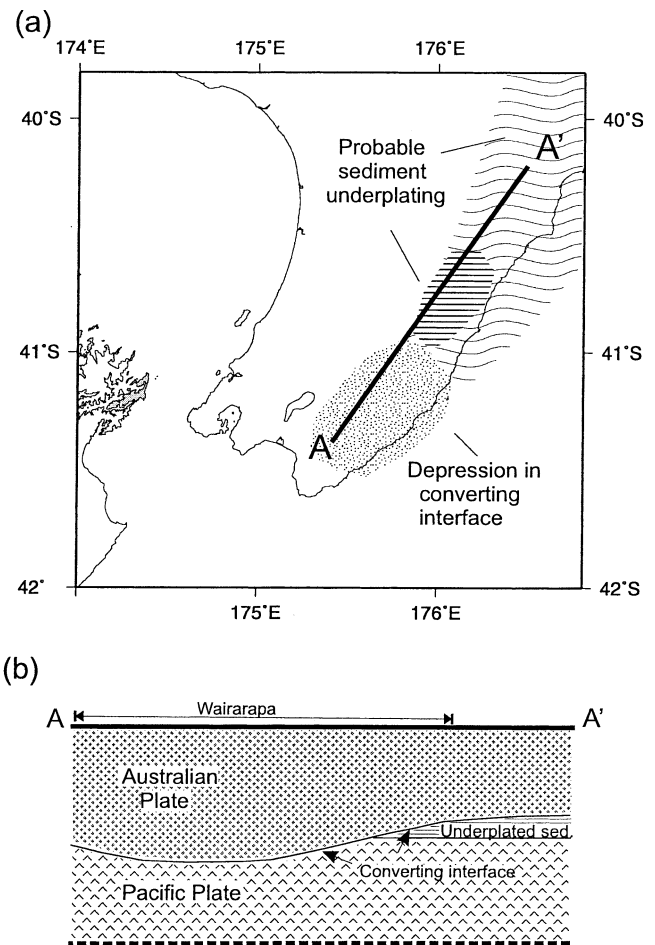


Figure 12. (a) Sediment distribution at the plate–plate interface. The denser horizontal shading corresponds to the subducted sediment indicated by the results of this work. The lighter shading shows the extension of the subducted sediment wedge proposed by Smith *et al.* (1989) and Walcott (1987). Line A–A' indicates the location of the section in (b). (b) A sketch section along the strike of the subducting plate at shallow depth showing the relation between the depression in the converting interface and the likely region of underplated sediment. Topography and sediment thickness are exaggerated for clarity.

from low to high velocity (see the previous section) points to the base of the overriding plate as the converting interface.

6 DISCUSSION

Many of the hypocentres solved for in this work are located, or have been relocated, below the converting interface or the upper boundary of the subducted slab. There is a transition between a flatter crust exhibiting a single dense band of earthquakes to a more steeply dipping crust with two distinct bands of seismicity (Fig. 10). This transition occurs around $x=60$ in the coordinates used in this work, or approximately below the west coast of southern North Island. The two bands of the double seismic zone occur 12–16 km apart. The thickness of the subducted slab at this point is therefore 16 km (± 2 km).

Ansell & Smith (1975) made a study of a small number of carefully relocated slab earthquakes with hypocentres down-dip of the central volcanic zone. These have been interpreted as showing a slab thickness of 9 km at a depth of approximately

200 km (Davy & Wood 1994). This thickness implies 'normal' subducted oceanic crust and provides the maximum limit of subduction for the anomalous crust further north (Fig. 13).

The thickness of the plateau off the east coast of North Island varies between 10 km in the north and 15 km in the south, adjacent to the Chatham Rise (Davy & Wood 1994). It is likely that the anomalous oceanic crust of the Hikurangi margin has been subducted at least as far as the westernmost side of the study area. This is consistent with the recent tectonic reconstruction of Luyendyk (1995) whereby crust is captured by the Pacific plate. The approximate position at 40 Ma is shown in Fig. 13(a) as the thickened area of captured crust rotated towards the Tonga–Kermadec subduction zone. By this time subduction along this margin of the Pacific plate had extended to the New Zealand block. This rotation continued, and by 20 Ma the Hikurangi Plateau was beginning to be subducted under the North Island (Fig. 13b). The trench-normal component of the oblique subduction direction eventually brought the plate towards its current position with the edge of the Hikurangi Plateau as shown in Fig. 13(c). Lineations, originally parallel to the spreading centre adjacent to the Cretaceous trench at the time of crust capture, are preserved in the Hikurangi plateau (Luyendyk 1995): their orientation at the present time is further evidence of such a mechanism for the formation of the Hikurangi margin and its current, partially subducted position.

The subduction of a complex region of thicker, more buoyant, oceanic crust partially accounts for several features observed along the Hikurangi margin.

(i) Enhanced uplift is seen along the Hikurangi margin on land (Walcott 1987; Smith *et al.* 1989). The thicker crust is more resistant to subduction and exerts a greater upward force than normal subducting oceanic crust.

(ii) The relatively flat angle of the upper part of the subducted slab (Ansell & Bannister 1996, and this study) is accounted for by the buoyancy of the anomalous crust.

(iii) There is a bend in the Kermadec subduction zone as it joins the Hikurangi Trough. The normal oceanic crust of the southern end of the Kermadec trench subducts more easily than the thicker, anomalous crust of the Hikurangi margin

(Fig. 1). At this point, the overriding plate changes from oceanic to thin, continental in character, which further contributes to the change in dynamics at the subduction interface.

The relative lack of a defined trench associated with the Hikurangi margin is explained since the buoyant anomalous crust has a lesser tendency to 'roll back' than normal oceanic crust. The trench is easily filled with sediment from the adjacent uplifting continental regions.

In a partially coupled subduction zone, the interplay between the lower surface of the overriding plate and topography on the subducting plate is a major control on the distribution of subducted sediment. Recent compression or variations in accretion/uplift along the strike of subduction would be required to create variations in the depth (or 'topography on the underside') of the overriding plate. The change in trend of the Hikurangi Trough at around 41°S (Chanier *et al.* 1999) and partitioned strain distribution in the overriding plate (Barnes *et al.* 1998; Barnes & de Lepinay 1997) provide starting points for plausible mechanisms. Alternatively, a change in Pacific plate motion 3–6 Ma has been proposed by Wessel & Kroenke (2000). They conclude that the transpression observed along the Alpine fault zone (South Island) results from this change. If this is the case, then a change in relative plate motion would also have taken place at the Hikurangi margin, increasing the trench-parallel component of subduction. Such forces could cause deformation in the subducting plate.

A refraction seismic experiment was carried out along the Hikurangi margin down the east coast of southern North Island (Chadwick 1996). The plate interface was modelled as a low-velocity thrust zone, approximately 5 km thick. The interpretation of Chadwick (1996) is therefore similar to the findings described in this paper for the region north of the observed depression in the converging interface, although the sediment layer that we infer, at 2–4 km, is not as thick. Chadwick (1996) finds that the low-velocity zone at the plate interface extends southwards, through the study region of this paper. This is not found in our model; in addition, we expect that a low-velocity zone of this kind would give rise to more high-amplitude converted phases than are observed in this area. It is possible that the low-velocity zone exists, but the

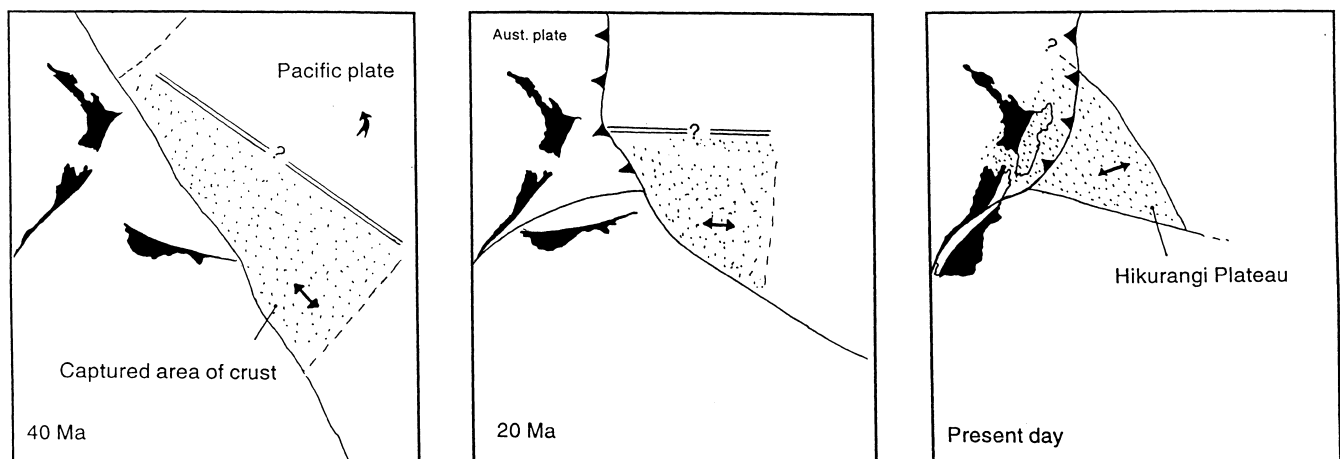


Figure 13. The development and subduction of the Hikurangi Plateau anomalous oceanic crust (shown as the stippled area) over time. The relative location of tectonic elements is taken from Luyendyk (1995) and the plate rotation vectors from Walcott (1987). The double-headed arrow gives the orientations of gravity lineations shown in Fig. 2 and observed at present on the Hikurangi Plateau. The right-hand figure shows the maximum limit of subducted anomalous crust constrained by Davy & Wood (1994) and the minimum limit constrained by this study.

interface is gradual, and does not lead to phase conversions of the amplitude observed further north. It is also possible that the source radiation pattern and source–receiver geometry together lead to low converted phase amplitude relative to the direct arrivals. Deep crustal velocities, below the plate interface zone, modelled by Chadwick (1996) are in good agreement with this work. The northernmost section modelled by Eberhart-Phillips & Reyners (1997) corresponds to the southern edge of the study area in this paper. Modelled seismic velocities are similar in both studies but Eberhart-Phillips & Reyners (1997) also determine values for the mantle under the subducted plate, deeper than is determined in this paper. This shows the subducting plate as a low-velocity feature extending into the mantle, as would be expected from the anomalous nature of the crust.

Finally, we note that submarine recordings of earthquakes are now possible following recent advances in three-component ocean-bottom seismometer technology. These data allow converted phase methods to be extended to the study of subduction zones not located near large land-masses. Converted-mode energy is also observed on arrivals from teleseismic distances; these are the subject of continued work at the University of Leeds.

7 CONCLUSIONS

The method outlined in this paper, developed through the investigation of the lithosphere beneath the Tararua and Wairarapa regions of southern North Island, New Zealand, provides a valuable means of using the extra information contained in converted phase arrivals. The multiphase approach has much potential in the investigation of Earth structure when used to map deep discontinuities, relocate earthquakes and investigate low-velocity layers as well as determining seismic velocity. Using converted phases has provided new information on the topography of the plate interface in addition to that provided by direct phases alone.

The following conclusions may be drawn regarding the shallow subduction zone structure of the Hikurangi margin in southern North Island, New Zealand.

(i) There is no evidence for subducted sediment at the converting interface across the Tararua region. In the northern Wairarapa the high incidence of converted phases suggests that this is the southernmost extremity of underplated sediments of thickness >2 km.

(ii) Topography on the converting interface shows that the plate boundary changes down-dip (southeast to northwest) from a shallow-dipping horizon with a slightly depressed region in the centre of the study area to a more steeply dipping interface.

(iii) The Pacific crust being subducted is anomalously thickened. Its high buoyancy, in comparison with standard oceanic crust, contributes to the unusual features of the Hikurangi subduction zone.

ACKNOWLEDGMENTS

The Leeds Tararua array was installed as part of the POMS project (NERC grant GR3/7699) This work was performed while AMR held a NERC PhD studentship and WM was supported by AMOCO (UK) under contract No. RAD 23(90). We are grateful for assistance and loan of equipment from

the Victoria University of Wellington, the New Zealand Institute of Geological and Nuclear Sciences and the UK NERC Geophysical Equipment Pool. Dave Francis and Mark Chadwick are thanked for their key roles in data acquisition and archiving. Two anonymous reviews are thanked for their suggestions in improving the clarity of the manuscript.

REFERENCES

- Aki, K. & Richards, P., 1980. *Quantitative Seismology: Theory and Methods*, Vol. 1, W.H. Freeman, San Francisco, CA.
- Ansell, J. & Bannister, S., 1996. Shallow morphology of the subducted Pacific plate along the Hikurangi margin, New Zealand, *Phys. Earth planet. Inter.*, **93**, 3–20.
- Ansell, J. & Smith, E., 1975. Detailed structure of a mantle seismic zone using the homogeneous station method, *Nature*, **253**, 518–520.
- Bannister, S., 1988. Microseismicity and velocity structure in the Hawke's Bay region New Zealand: fine structure of the subducting Pacific plate, *Geophys. J.*, **95**, 45–62.
- Barnes, P. & de Lepinay, B.M., 1997. Rates and mechanics of rapid frontal accretion along the very obliquely convergent southern Hikurangi Margin, New Zealand, *J. geophys. Res.*, **102**, 24 931–24 952.
- Barnes, P., de Lepinay, B.M. & Jean-Yves Collot, J.D., 1998. Strain partitioning in the transition area between oblique subduction and continental collision, Hikurangi Margin, New Zealand, *Tectonics*, **17**, 534–557.
- Bradshaw, J.D., 1989. Cretaceous geotectonic patterns in the New Zealand region, *Tectonics*, **8**, 803–820.
- Bray, T., 1991. The determination of the velocity structure in the upper mantle by seismic traveltimes inversion, *PhD thesis*, University of Cambridge, Cambridge.
- Brisbourne, A., Stuart, G. & Kendall, J., 1999. Anisotropic structure of the Hikurangi subduction zone, New Zealand—integrated interpretation of surface-wave and body-wave data, *Geophys. J. Int.*, **137**, 214–230.
- Chadwick, M., 1996. Structure along the shallow part of a subduction zone: Palliser Bay to Hawkes Bay refraction experiment, New Zealand, *PhD thesis*, Victoria University, Wellington.
- Chanier, F., Ferriere, J. & Angelier, J., 1999. Extensional deformation across an active margin, relations with subsidence, uplift and rotations: The Hikurangi subduction, New Zealand, *Tectonics*, **18**, 862–876.
- Davy, B. & Wood, R., 1994. Gravity and magnetic modelling of the Hikurangi Plateau, *Mar. Geol.*, **118**, 139–151.
- de Boor, C., 1972. On calculating with B-splines, *J. Approx. Theory*, **6**, 50–62.
- Eberhart-Phillips, D. & Reyners, M., 1997. Continental subduction and three-dimensional crustal structure: the northern South Island, New Zealand, *J. geophys. Res.*, **102**, 11 843–11 861.
- Eberhart-Phillips, D. & Reyners, M., 1999. Plate interface properties in the northeast Hikurangi subduction zone, New Zealand, from converted seismic waves, *Geophys. Res. Lett.*, **26**, 2565–2568.
- Franklin, J., 1970. Well-posed stochastic extensions of ill-posed linear problems, *J. math. Anal. Appl.*, **31**, 682–716.
- Gledhill, K. & Stuart, G., 1996. Seismic anisotropy in the fore-arc region of the Hikurangi subduction zone, New Zealand, *Phys. Earth planet. Inter.*, **95**, 211–225.
- Gubbins, D., Barnicoat, A. & Cann, J., 1994. Seismological constraints on the gabbro-eclogite transition in subducted oceanic crust, *Earth planet. Sci. Lett.*, **122**, 89–101.
- Helfrich, G. & Stein, S., 1993. Study of the structure of the slab–mantle interface using reflected and converted seismic waves, *Geophys. J. Int.*, **115**, 14–40.
- Helfrich, G., Stein, S. & Wood, B.J., 1989. Subduction zone thermal structure and mineralogy and their relationship to seismic wave reflections and conversions at the slab/mantle interface, *J. geophys. Res.*, **94**, 753–763.

- Iidaka, T., Mizoue, M., Nakamura, I., Tsukuda, T., Sakai, K., Kobayasi, M., Haneda, T. & Hashimoto, S., 1990. The upper boundary of the Philippine Sea plate beneath the western Kanto region estimated from S-P converted waves, *Tectonics*, **179**, 321–326.
- Lancaster, P. & Salkauskas, K., 1986. *Curve and Surface Fitting: An Introduction*, Academic Press, London.
- Lodge, R., Steblov, G. & Gubbins, D., 1999. Fundamental leaking mode (PL) propagation along the Tonga–Kermadec–Hikurangi–Macquarie margin, *Geophys. J. Int.*, **137**, 675–690.
- Luyendyk, B., 1995. Hypothesis for Cretaceous rifting of East Gondwana caused by subducted slab capture, *Geology*, **23**, 373–376.
- Mao, W. & Stuart, G., 1997. Rapid ray tracing for multi-wavetype tomography in complex 2-D and 3-D isotropic media, *Geophysics*, **62**, 298–308.
- Marson-Pidgeon, K., Savage, M.K., Gledhill, K. & Stuart, G., 1999. Seismic anisotropy beneath the lower half of North Island, New Zealand, *J. geophys. Res.*, **104**, 20 277–20 286.
- Powell, M., 1991. *Approximation Theory and Methods*, Cambridge University Press, Cambridge.
- Reading, A.M., 1996. Deep lithospheric structure from multi-phase tomography: the subduction zone beneath southern North Island, New Zealand, *PhD thesis*, University of Leeds, Leeds.
- Reading, A.M., Mao, W. & Gubbins, D., 2001. Polarization filtering for automatic picking of seismic data and improved converted phase detection, *Geophys. J. Int.*, **147**, 227–234 (this issue).
- Robinson, R., 1986. Seismicity, structure and tectonics of the Wellington region, *Geophys. J. R. astr. Soc.*, **87**, 379–409.
- Samson, J.C. & Olson, J.V., 1981. Data-adaptive polarization filters for multichannel geophysical data, *Geophysics*, **46**, 1423–1431.
- Smith, E.G.C., Stern, T. & Reyners, M., 1989. Subduction and back-arc activity at the Hikurangi convergent margin, New Zealand, *Pure appl. Geophys.*, **129**, 203–231.
- Smith, G., Gubbins, D. & Mao, W., 1994. Fast P-wave propagation in subducted Pacific lithosphere—refraction from the plate, *J. geophys. Res.*, **99**, 23 787–23 800.
- Smith, W.D., 1970. S to P conversion as an aid to crustal studies, *Geophys. J. R. astr. Soc.*, **19**, 513–519.
- Spencer, C. & Gubbins, D., 1980. Travel-time inversion for simultaneous earthquake location and velocity structure determination in laterally varying media, *Geophys. J. R. astr. Soc.*, **63**, 95–116.
- Stuart, G., Francis, D., Gubbins, D. & Smith, G., 1995. Tararua broadband array, North Island, New Zealand, *Bull. seism. Soc. Am.*, **85**, 325–333.
- Walcott, R., 1987. Geodetic strain and the deformational history of the North Island of New Zealand during the late Cainozoic, *Phil. Trans. R. Soc. Lond.*, **321**, 231–277.
- Wessel, P. & Kroenke, L.W., 2000. Ontong Java plateau and late Neogene changes in Pacific plate motion, *J. geophys. Res.*, **105**, 28 255–28 277.
- Wood, R. & Davy, B., 1994. The Hikurangi Plateau, *Mar. Geol.*, **118**, 153–173.